BJP British Journal of Pharmacology

DOI:10.1111/j.1476-5381.2011.01497.x
www.brjpharmacol.org

Themed Section: Cannabinoids in Biology and Medicine, Part II

RESEARCH PAPER

Δ^9-Tetrahydrocannabinol and *N*-arachidonyl glycine are full agonists at GPR18 receptors and induce migration in human endometrial HEC-1B cells

Douglas McHugh[1], Jeremy Page[1], Emily Dunn[1] and Heather B Bradshaw[1,2]

[1]*Department of Psychological and Brain Sciences, Indiana University, Bloomington, IN, USA, and* [2]*Kinsey Institute for the Study of Sex, Gender and Reproduction, Indiana University, Bloomington, IN, USA*

Correspondence
Heather B Bradshaw, Assistant Professor, Department of Psychological and Brain Sciences, Indiana University, 1101 E. 10th Street, Bloomington, IN 47405, USA. E-mail: hbbradsh@indiana.edu

Keywords
GPR18; NAGly; endometriosis; abnormal cannabidiol receptor; cellular migration; THC

Received
22 December 2010
Revised
15 April 2011
Accepted
29 April 2011

BACKGROUND AND PURPOSE

Endometriosis is a disorder in which the endometrium forms growths outside the uterus and is associated with chronic pain. Recent evidence suggests that endometrial motility plays a role in the aetiology of endometriosis. The endocannabinoid system regulates cellular migration. Given the growing involvement of the endocannabinoids in reproduction, we investigated the role of the endocannabinoid system in migration of endometrial cells.

EXPERIMENTAL APPROACH

Migration of the human endometrial HEC-1B cells was assayed. Standard PCR techniques were used to determine the presence of the GPCR, GPR18, in HEC-1B cells, and p44/42 MAPK was assayed in stably transfected HEK293-GPR18 cells to determine receptor specificity for known cannabinoid agonists and antagonists. *N*-arachidonoyl ethanolamine (AEA) metabolism was measured, using HPLC/MS/MS for lipid analysis.

KEY RESULTS

AEA, Δ^9-tetrahydrocannabinol (Δ^9-THC) and *N*-arachidonoyl glycine (NAGly) induce migration of HEC-1B cells through cannabinoid CB_1 receptor-independent mechanisms. MAPK activation in HEK293-GPR18 cells revealed novel pharmacology for known CB_1 and CB_2 receptor ligands at GPR18 receptors, including Δ^9-THC, which activates MAPK at nanomolar concentrations, whereas WIN 55212-2, CP55940, JWH-133 and JWH-015, and arachidonyl-1-hydroxy-2-propylamide (R1-methanandamide) had no effect. Moreover, HEC-1B migration and MAPK activation by NAGly and Δ^9-THC were antagonized by *Pertussis* toxin, AM251 and cannabidiol.

CONCLUSIONS AND IMPLICATIONS

An understanding of the function and regulation of GPR18 and its molecular interactions with endogenous ligands, and how phytocannabinoids play a role with GPR18 signalling is vital if we are to comprehensively assess the function of the cannabinoid signalling system in human health and disease.

LINKED ARTICLES

This article is commented on by Alexander, pp. 2411–2413 of this issue and is part of a themed section on Cannabinoids in Biology and Medicine. To view Alexander visit http://dx.doi.org/10.1111/j.1476-5381.2011.01731.x. To view the other articles in this section visit http://dx.doi.org/10.1111/bph.2012.165.issue-8. To view Part I of Cannabinoids in Biology and Medicine visit http://dx.doi.org/10.1111/bph.2011.163.issue-7

Abbreviations

Abn-CBD, abnormal cannabidiol; ACPA, N-(cyclopropyl)-5Z,8Z,11Z,14Z-eicosatetraenamide; AEA, *N*-arachidonoyl ethanolamine; 2-AG, 2-arachidonoyl glycerol; AM251, 1-(2,4-dichlorophenyl)-5-(4-iodophenyl)-4-methyl-N-(1-piperidyl)pyrazole-3-carboxamide; CBD, cannabidiol; CP55,940, 2-[(1R,2R,5R)-5-hydroxy-2-(3-hydroxypropyl) cyclohexyl]-5-(2-methyloctan-2-yl)phenol; Δ9-THC, Δ^9-tetrahydrocannabinol; DMEM, Dulbecco's modified Eagle's medium; DMSO, dimethyl sulphoxide; FAAH, fatty acid amide hydrolase; FBS, fetal bovine serum; JWH-015, [(6aR,10aR)-6,6-dimethyl-3-(2-methyloctan-2-yl)-6a,7,10,10a-tetrahydrobenzo[c]chromen-9-yl]methanol; JWH-133, (6aR,10aR)-3-(1,1-dimethylbutyl)-6a,7,10,10a-tetrahydro-6,6,9-trimethyl-6H-dibenzo[b,d]pyran; NAGly, *N*-arachidonoyl glycine; O-1602, *trans*-4-[3-methyl-6-(1-methylethenyl)-2-cyclohexen-1-yl]-5-methyl-1,3-benzenediol; O-1918, 1,3-dimethoxy-5-methyl-2-[(1R,6R)-3-methyl-6-(1-methylethenyl)-2-cyclohexen-1-yl]-benzene; PTX, *Pertussis* toxin; R1-methAEA, (R)-(+)-arachidonyl-1′-hydroxy-2′-propylamide; Rimonabant (SR141716A), *N*-(piperidin-1-yl)-5-(4-chlorophenyl)-1-(2,4-dichlorophenyl)-4-methyl-1*H*-pyrazole-3-carboximide hydrochloride; SR144528, 5-(4-chloro-3-methylphenyl)-1-[(4-methylphenyl)methyl]-*N*-[(1*S*,4*R*,6*S*)-1,5,5-trimethyl-6bicyclo[2.2.1]heptanyl]pyrazole-3-carboxamide; WIN55212-2, (R)-(+)-[2,3-dihydro-5-methyl-3-(4-morpholinylmethyl)pyrrolo[1,2,3-de]-1,4-benzoxazin-6-yl]-1-napthalenylmethanone

Introduction

Healthy endometrium undergoes rapid and varied phenotypic changes to mediate the dynamic proliferation, secretion and regression events associated with the phases of the hormonal cycle. These extensive phenotypic changes are a unique characteristic of endometrium and their dysregulation likely plays a role in the myriad of disorders associated with this tissue. Here we have studied endometriosis, a condition where the endometrium, which normally provides the inner lining of the uterus, grows in other areas of the body, typically on the ovaries, bowel, rectum, bladder and pelvic lining. It is a leading cause of chronic recurring pelvic pain, dysmenorrhoea (painful menstruation) and infertility in millions of women of reproductive age (Bulletti *et al.*, 2010). The precise pathogenesis of endometriosis is unknown, but the disorder does exhibit a positive correlation with estrogens and symptom severity is often synchronous with the menstrual cycle. Proposed explanations for the development of endometriosis favour mechanisms that allow endometrial cells to exit the uterine cavity, implant in other tissues and proliferate. Therefore, cell motility, adhesion and proliferation are phenotypes of endometrium that are especially relevant to endometriosis; however, the exact cellular signalling involved in driving these changes is poorly understood. Here, we show that the endogenous cannabinoid (endocannabinoid) system is part of the regulatory system that stimulates human endometrial migration and suggest that a dysregulation of this system plays a role in pathophysiologies of the uterus.

Anandamide (*N*-arachidonoyl ethanolamine; AEA) is an endogenous lipid produced throughout the body and was identified as the first endocannabinoid, activating the cannabinoid CB_1 and CB_2 receptors (Devane *et al.*, 1992; receptor nomenclature follows Alexander *et al.*, 2011). In the mouse, uterine AEA production varies according to state of pregnancy, uterine receptivity and embryo implantation (Schmid *et al.*, 1997; Sun and Dey, 2008). Fatty acid amide hydrolase (FAAH), the principal inactivating enzyme for AEA, is also active in the mouse uterus (Maccarrone *et al.*, 2000), localized in the endometrial epithelium. Down-regulation of this FAAH activity has been shown in early pregnancy (Maccarrone *et al.*, 2002) and over the oestrous cycle in rats and mice, suggesting a role for hormonal regulation of this enzyme and thus on signalling in the endocannabinoid system (Xiao *et al.*, 2002; Klinger *et al.*, 2006). FAAH also controls one of the two distinct biosynthetic pathways for the formation of *N*-arachidonoyl glycine (NAGly) from AEA. (Burstein *et al.*, 2000; Bradshaw *et al.*, 2009). Like AEA, NAGly is produced throughout the body (Huang *et al.*, 2001; Bradshaw *et al.*, 2009) but, unlike AEA, it has no activity at either CB_1 or CB_2 receptors (Sheskin *et al.*, 1997). We have demonstrated that NAGly production in the uterus varies with the hormonal cycle, suggesting a role for NAGly in uterine physiology (*Bradshaw and Allard, unpublished experiments*).

The CB_1 and CB_2 receptors, which are $G_{i/o}$-GPCRs, modulate cell migration (Derocq *et al.*, 2000; Song and Zhong, 2000; Walter *et al.*, 2003). Stimulation of both neurons and microglia selectively increased production of the endocannabinoid, 2-arachidonoyl glycerol (2-AG), which, together with other related lipids, triggered microglial cell migration by activating CB_2 and the abnormal cannabidiol (Abn-CBD) receptors (Walter *et al.*, 2003). Also, NAGly potently induced concentration-dependent migration of immortalized microglia, more effectively than any previously described cannabinoid ligands (McHugh *et al.*, 2010). The agonist profile of the $G_{i/o}$-coupled Abn-CBD receptor characteristically includes activation by Abn-CBD and O-1602, compounds inactive at CB_1 and CB_2 receptors (Begg *et al.*, 2003; Mackie and Stella, 2006). Other agonists include 2-AG and AEA (Járai *et al.*, 1999; Wagner *et al.*, 1999; Walter *et al.*, 2003). Migration assays with wildtype HEK293 and cells stably transfected with the GPCR, GPR18 support our working hypothesis that NAGly is acting via $G_{i/o}$-coupled GPR18 receptors (Kohno *et al.*, 2006; McHugh *et al.*, 2010). Abn-CBD and O-1602 also induce migration of GPR18-transfected cells but not wildtype cells, suggesting that GPR18 is a receptor target for Abn-CBD (McHugh *et al.*, 2010). Significantly, NAGly-induced migration in GPR18-transfected cells is blocked by O-1918, arachidonoyl serine and cannabidiol (CBD), which are weak partial agonists/antagonists of the Abn-CBD receptor (McHugh *et al.*, 2010).

Up-regulation of genes associated with 'migration-capable' cell phenotypes occurs in late secretory phase endometrial tissue (Talbi *et al.*, 2006). Human endometrial cells and the derived endometrial cell lines, HEC-1A and

HEC-1B migrate *in vitro* towards oestrogen (Fujimoto *et al*. 1996; Acconcia *et al*., 2006). This capacity of human endometrial cells to migrate in response to oestrogen relates to the oestrogen-dependence of endometriosis (Kitawaki *et al*., 2002). If oestrogen is a chemoattractant for human endometrial cells and endometriosis symptoms are positively correlated with oestrogen availability, chemotaxis may be a mechanism by which endometrial cells exit the uterus.

Here, using the HEC-1B human endometrial cell line, we have shown that AEA, Δ^9-tetrahydrocannabinol (Δ^9-THC) and NAGly potently induced migration of human endometrial cells through a CB_1 receptor-independent mechanism. We have also tested the hypothesis that NAGly acted through GPR18 in both HEC-1B and in an overexpressing GPR18-transfected HEK293 cell line. MAPK activation assays in HEK293-GPR18 cells disclosed a novel pharmacology for some established CB_1 and CB_2 receptor ligands at GPR18 receptors, including Δ^9-THC, which activated MAPK at nanomolar concentrations. Furthermore, HEC-1B migration and MAPK activation by NAGly and Δ^9-THC were antagonized by AM251, CBD and *Pertussis* toxin (PTX), adding to the novel cannabinoid pharmacology revealed at GPR18.

Methods

Cells in culture

HEK293 wildtype (ATCC, Manasses, VA, USA) and HEK293 cells stably transfected with GPR18 [HEK293-GPR18; generated as previously described (McHugh *et al*., 2010)], CB_1 (HEK293-CB_1; a kind gift from Dr Ken Mackie, Indiana University) and CB_2 (HEK293-CB_2; a kind gift from Dr Ken Mackie, Indiana University) were grown in high-glucose DMEM (Gibco, Carlsbad, CA, USA) supplemented with FBS (10%), penicillin (100 units·mL^{-1}), streptomycin (100 μg·mL^{-1}), and passaged every 4–5 days for a maximum of 30 passages. Twenty-four hours prior to experimentation, the culture media for the HEK293 wildtype, HEK293-GPR18, HEK293-CB_1 and HEK293-CB_2 cells was replaced by serum-free high-glucose DMEM (Gibco) supplemented with penicillin (100 units·mL^{-1}),and streptomycin (100 μg·mL^{-1}). Similarly, the human endometrial cell line HEC-1B (ATCC) was grown in high-glucose DMEM (Gibco) supplemented with FBS (10%), penicillin (100 units·mL^{-1}), streptomycin (100 μg·mL^{-1}), and passaged every 4–5 days for a maximum of 30 passages. Twenty-four hours prior to experimentation, the culture media for the HEC-1B cells was replaced by phenol red-free and serum-free high-glucose DMEM (Gibco) supplemented with penicillin (100 units·mL^{-1}) and streptomycin (100 μg·mL^{-1}).

Migration assay

In vitro cell migration assays were performed using a modified 96-well Boyden Chamber and PVP-free polycarbonate filters with 10 μm diameter pores (Neuroprobe Inc., Gaithersburg, MD, USA), which are shown as the clear unstained circles in the photographed filters (Figure 1B). The upper wells of the Boyden chamber were filled with 50 μL of suspension of 1×10^6 cells·mL^{-1} in serum-free DMEM, before incubation with a 5% CO_2 atmosphere at 37°C for 3 h. Following incubation, non-migrated cells were then removed before fixation and staining with Diff Quik® stain set. Finally, the filter was sectioned and mounted onto microscope slides and the migrated cells counted in 10 non-overlapping fields (×40 magnification) with a light microscope by several workers, without knowledge of the treatments. For inhibition of induced migration, cells were pre-incubated with antagonist for 30 min at 37°C in a water bath before loading into the upper wells; the lower wells contained the equivalent concentration of antagonist and test compound to ensure that the only concentration gradient present is that generated by the test compound.

Mass spectrometric analysis of deuterium-labelled AEA metabolism

Recovery of deuterium-labelled AEA (d_4AEA) and NAGly (d_0NAGly and d_2NAGly) was measured after incubation with HEC-1B cells at four time points (5, 15, 90 and 180 min), using HPLC/MS/MS, as previously described by Bradshaw *et al*., (2009).

Isolation of total RNA and PCR for GPR18

RNA was extracted from HEC-1B cells using the RNAqueous® small-scale phenol-free total RNA isolation kit (Applied Biosystems, Carlsbad, CA, USA) and RNA samples (2 μg) were reverse transcribed using the SuperScript II™ Reverse Transcription Kit (Invitrogen, Carlsbad, CA, USA). Expression of GPR18 in HEC-1B was determined by PCR using oligonucleotide primers based on the sequence of the *Mus musculus* GPR18 mRNA (GenBank Accession No. NM_182806.1). The primer sequences used were forward, TGAAGCCCAAGGTCA AGGAGAAGT and reverse, TTCATGAGGAAGGTGGTGAAG GCT (amplicon 163 bp) for GPR18. PCR reactions were subjected to an initial HotStart Taq DNA polymerase activation step of 95°C for 7 min, followed by 40 cycles of 94°C for 30 s, 55°C for 30 s and 72°C for 30 s. PCR products were analysed on a 2% agarose gel with ethidium bromide. Single bands corresponding to 163 bp for the GPR18 amplicon were recorded.

In-Cell Western assay to quantify MAPK phosphorylation

An In-Cell Western assay was employed to simultaneously detect both the phosphorylated MAPK protein and normalize for total MAPK protein. The following primary antibodies were used to detect endogenous levels of the relevant total MAPK and phosphorylated MAPK: p44/42 MAPK rabbit pAb, and phospho-p44/42 MAPK mouse mAb (#4695 and #9106; Cell Signaling Technology). Cells were plated into 96-well plates coated with 1 μg·mL^{-1} poly-D-lysine and treated with vehicle (Vh) (0.1% DMSO) or test compound (0.1 nM–100 μM) for 5 min. Ionomycin (10 μM) treatment was used as a positive control. Upon completion of the drug treatments, an In-Cell Western assay was conducted as previously described (McHugh *et al*., 2010).

Analysis of data

All data are expressed as means ± SEM and n = number of independent experiments. For HEC-1B endometrial cells, the mean number of cells migrated in response to test compounds was normalized against the mean number of migrated cells elicited by 1 nM oestradiol (in 0.1% DMSO),

corrected for the number of cells migrating with vehicle (0.1% DMSO) was subtracted. For HEK293 wildtype, HEK293-CB_1, HEK293-CB_2, and HEK293-GPR18 transfected cell MAP kinase activation assays, the test compound responses were normalized against the mean effect elicited by 10 μM of the calcium ionophore, ionomycin. Concentration-response curves were generated using a sigmoidal dose-response (variable slope) curve-fitting process. The apparent K_B value of CBD for antagonism of Δ^9-THC was calculated by substituting a single concentration ratio value into the equation: $[x - 1] = B/K_B$, where x (the 'concentration ratio') is the EC_{50} value of Δ^9-THC in the presence of CBD at a concentration, B, divided by the EC_{50} value of Δ^9-THC alone (Tallarida and Jacob, 1979). Statistical analyses were performed with GraphPad Prism 4; using one-way ANOVA with Dunnett's *post hoc* tests; $P < 0.05$ was considered to show significance.

Materials

High-glucose Dulbecco's modified Eagle's medium (DMEM), high-glucose, phenol red-free DMEM, penicillin, streptomycin, dimethyl sulphoxide (DMSO), poly-D-lysine, ionomycin, DPX mountant Tween-20, Triton X-100, phosphate buffered saline, 17β-oestradiol from Sigma-Aldrich (St. Louis, MO, USA); fetal bovine serum (FBS) from Lonza, (Houston, TX, USA); Diff-Quik® from VWR, (Bridgeport, NJ, USA); methanol, 37% formaldehyde from Fisher Scientific, (Pittsburg, PA, USA); Odyssey Blocking buffer, goat anti-mouse 680 nm antibody (926-32220), goat anti-rabbit 800 nm antibody (926-32211) from Li-Cor (Lincoln, NE, USA); p44/42 MAPK rabbit polyclonal antibody (#4695) and phospho-p44/42 MAPK mouse monoclonal antibody (#9106) from Cell Signaling Technology (Danvers, MA, USA); NAGly, AEA, N-(cyclopropyl)-eicosatetraenamide (ACPA), WIN 55212-2, CP55,940 and AM251 from Enzo Life Sciences (Farmingdale, NY, USA); Abn-CBD, O-1602, SR141716A (rimonabant) SR144528, (R)-arachidonyl-1′-hydroxy-2′-propylamide (R1meth-AEA) and the deuterium labelled AEA and NAGly used as standards were supplied by Cayman Chemicals (Ann Arbor, MI, USA). JWH-133 and JWH-015 were kind gifts from Dr John Huffman, (Clemson University). Δ^9-THC and CBD were from the National Institute on Drug Abuse.

Results

HEC-1B cell migration

We compared oestradiol-induced HEC-1B migration with NAGly and AEA over a concentration range of 0.1 nM to 10 μM. All three signalling lipids produced response curves with a bell-shaped pattern of induced migration beginning at sub-nanomolar concentrations, peaking in the low nanomolar range and then showing a decreased response trend towards high nanomolar/micromolar concentrations (Figure 1A). NAGly and AEA exhibited greater efficacy than oestradiol for inducing HEC-1B migration (Figure 1A,B).

The role of cannabinoid receptors was examined using SR141716A (rimonabant; CB_1 receptor antagonist/inverse agonist), SR144528 (CB_2 receptor antagonist/inverse agonist) and CBD (GPR18 receptor weak partial agonist/antagonist). HEC-1B cell migration to SR141716A (0.1 nM–10 μM) alone,

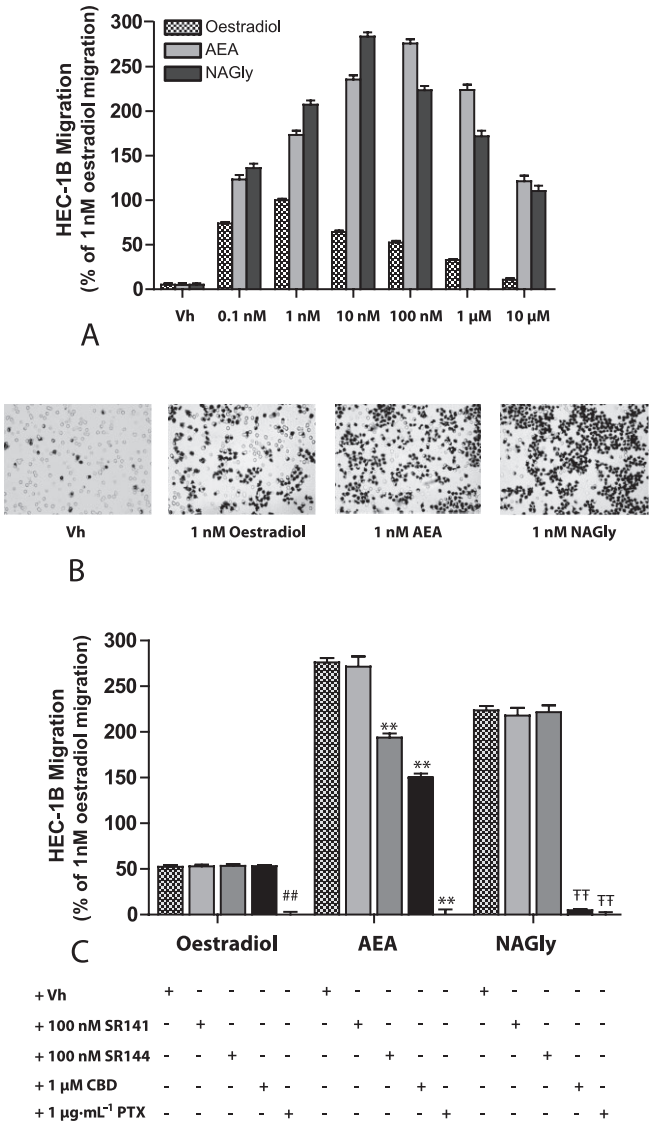

Figure 1

Oestradiol, AEA and NAGly induced HEC-1B endometrial cell migration. (A) HEC-1B cell migration in response to basal conditions; vehicle (vh; 0.1% DMSO); 0.1 nM–10 μM concentrations of oestradiol, AEA and NAGly; $n = 3$. (B) Filter photographs of one random field of view at ×40 magnification indicating the migration produced by the vehicle; 1 nM oestradiol, 1 nM AEA and 1 nM NAGly. The 10 μm diameter pores can be discerned as the clear unstained circles. (C) HEC-1B cell migration in response to 100 nM oestradiol + vehicle (0.1% DMSO), 100 nM oestradiol + 100 nM SR141716A (rimonabant), 100 nM oestradiol + 100 nM SR144528, 100 nM oestradiol + 1 μM CBD, 100 nM oestradiol + 1 μg·mL^{-1} PTX; 100 nM AEA + vehicle, 100 nM AEA + 100 nM SR141716A (rimonabant), 100 nM AEA + 100 nM SR144528, 100 nM AEA + 1 μM CBD, 100 nM AEA + 1 μg·mL^{-1} PTX; 100 nM NAGly + vehicle, 100 nM NAGly + 100 nM SR141716A (rimonabant),100 nM NAGly + 100 nM SR144528, 100 nM NAGly + 1 μM CBD, 100 nM NAGly + 1 μg·mL^{-1} PTX. ##$P <$ 0.01, significantly different from 100 nM oestradiol; **$P < 0.01$, significantly different from 100 nM AEA; ††$P < 0.01$, significantly different from 100 nM NAGly; one-way ANOVA; $n = 3$–6.

SR144528 (0.1 nM–10 μM) alone, and CBD (0.1 nM–10 μM) alone were not different from that to vehicle (0.1% DMSO) alone. SR141716A (100 nM) had no effect on oestradiol (100 nM), AEA (100 nM) or NAGly (100 nM). SR144528 (100 nM) significantly attenuated the response to AEA (100 nM) but not oestradiol (100 nM) or NAGly (100 nM). Similar to SR144528, CBD (1 μM) was able to significantly attenuate AEA (100 nM), but in addition, it completely blocked NAGly (100 nM) -induced migration of HEC-1B cells, without effect on oestradiol-induced migration (Figure 1C). PTX (1 $\mu g \cdot mL^{-1}$) pre-treatment abolished the migration to oestradiol, AEA and NAGly, without affecting cell viability (Trypan blue exclusion; data not shown).

AEA is metabolized into NAGly in HEC-1B cells through two biochemical pathways

In C6 glioma cells, NAGly is a product of AEA metabolism through a FAAH-dependent pathway and an alcohol dehydrogenase-dependent pathway (Bradshaw *et al.*, 2009). As FAAH activity had not been investigated in HEC-1B cells, we first measured the rates of deuterium-labelled AEA (d_4AEA) metabolism using HPLC/MS/MS (Figure 2A). After 1.5 h of incubation with HEC-1B cells, only ~10% of d_4AEA remained (Figure 2B) and HEC-1B cells produced both d_0NAGly and d_2NAGly, indicating that both of the 'AEA-to-NAGly' conversion pathways demonstrated in C6 glioma cells were present and functional in HEC-1B cells (Figure 2A,B). These data suggest that the effect of AEA on migration of HEC-1B cells may be, in part, due to its conversion to NAGly, which then activates GPR18.

PCR measurement of GPR18 mRNA

To determine if GPR18 receptors are produced by HEC-1B cells, we performed standard PCR techniques with the previously optimized GPR18 primers, verified in BV-2 microglia and GPR18-transfected HEK293 cells (McHugh *et al.*, 2010). Figure 3 shows the definitive band at 163bp that coincides with the primer product for GPR18 mRNA, demonstrating the presence of GPR18 mRNA in HEC-1B cells.

Evaluation of cannabinoid ligands at GPR18 through MAPK activation assays

We have proposed the working hypothesis that GPR18 is the molecular identity of the Abn-CBD receptor, (McHugh *et al.*, 2010) and showed that NAGly drove MAPK (p44/42; ERK1/2) activation in GPR18-transfected HEK293 cells. Here, we have used the same expression system to screen the specificity of cannabinoid ligands for CB_1 and CB_2 receptors, at GPR18 in HEK293 cells.

In order of potency, NAGly, O-1602, Abn-CBD, Δ^9-THC, AEA and ACPA activated GPR18 to induce p44/42 MAPK phosphorylation, as full agonists (Figure 4A) and their EC_{50} values are shown in Table 1. CBD was a weak GPR18 partial agonist, inducing p44/42 MAPK only at concentrations >10 μM (Figure 4B; EC_{50} value in Table 1).

WIN55212-2, CP55940, R1-methAEA, JWH-133 and JWH-015 had no effect on GPR18 receptors (Figure 4C). In HEK293-CB_1 cells, WIN55212-2, CP55940, R1-methAEA and ACPA-did activate p44/42 MAPK (Figure 4D; EC_{50} values in Table 1). Similarly, JWH-133 and JWH-033 were both full

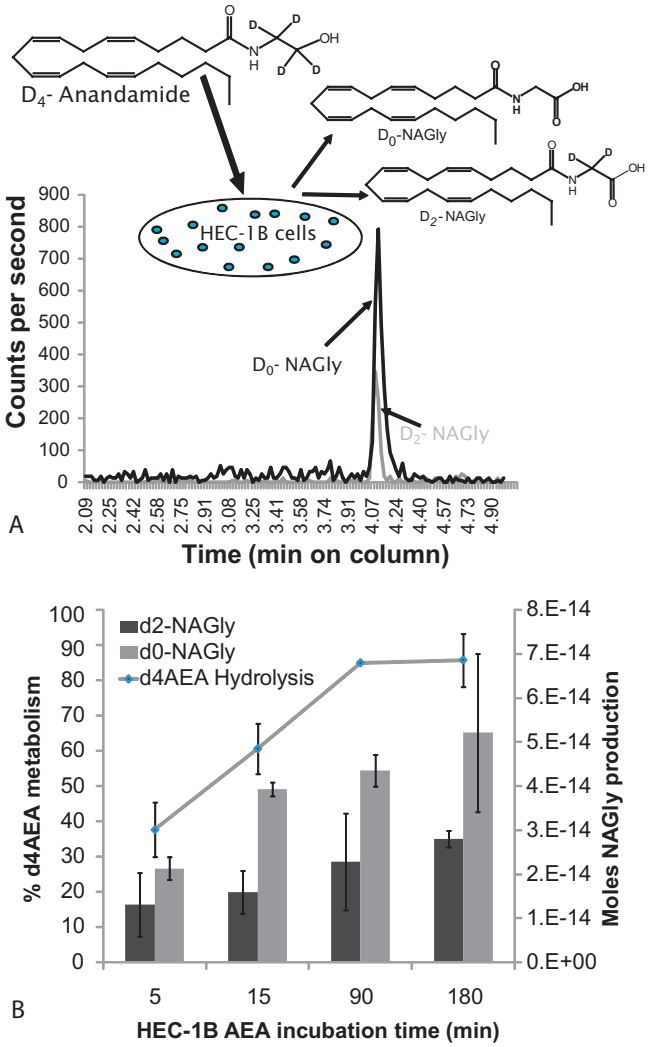

Figure 2

Deuterium-labelled anandamide is a precursor for NAGly in HEC-1B through two pathways. (A) Molecular structures of d_4-anandamide, d_0-NAGly and d_2-NAGly are illustrated. The NAGly products were formed after d_4-AEA was incubated with HEC-1B cells. The chromatogram shows the relative peaks of the d_0-NAGly and the d_2-NAGly products from a 90 min incubation of d_4-AEA. (B) The left hand axis represents the percentage of metabolism (the inverse of d_4-AEA recovery measured over time), whereas the right hand axis represents the level of two different NAGly products (d_0-NAGly and d_2-NAGly) measured at the same time points in the same experiments.

agonists to activate CB_2 receptor -induced p44/42 MAPK (EC_{50} values in Table 1; concentration–response curves not shown). Δ^9-THC had no effect on HEK293 wildtype cells (Figure 5B) nor did any of the other compounds tested (Table S1).

The most surprising of the outcomes centred on the novel pharmacological activity of Δ^9-THC at GPR18 receptors (Figure 4A). Given that both NAGly and Δ^9-THC were found to be full agonists at GPR18, and that our HEC-1B cell migration experiments demonstrated NAGly's effects were blocked by CBD, we next tested the ability of CBD to antagonize Δ^9-THC activity at GPR18. A concentration of 20 μM was chosen, which was below the observed threshold of GPR18

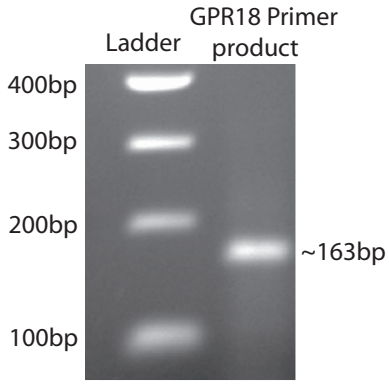

Figure 3

HEC-1B endometrial cells express GPR18 mRNA. Gel electrophoresis of HEC-1B endometrial cell RT-qPCR products. RT-qPCR products were collected from the RT-qPCR run; loading buffer was added to the samples, which were run on a 2% agarose gel.

activation for CBD (Figure 4B, Table 1). CBD (20 μM) caused a significant rightward shift in the concentration–response curve for Δ^9-THC-induced phosphorylation of p44/42 MAPK (Figure 5A). An apparent K_B value of 57.1 nM was calculated for CBD. It should be noted that CBD might not be acting competitively here. Concentrations of Δ^9-THC greater than 1 mM would be required to establish the E_{max} and ascertain this.

The data in Figure 5C demonstrate that AM251 was a very weak GPR18 partial agonist, able to induce p44/42 MAPK only at concentrations above 50 μM (EC_{50} value in Table 1). AM251 also antagonized Δ^9-THC (100 nM) and NAGly (100 nM) -induced p42/44 MAPK phosphorylation in HEK293-GPR18 cells with IC_{50} values of 47.4 nM and 143.8 nM respectively (Figure 5D).

Δ^9-THC drives HEC-1B migration and is blocked by CBD and AM251

We next sought to replicate these interesting findings with the HEC-1B cell migration assay. CBD and AM251 alone had no effect on HEC-1B cell migration, but Δ^9-THC exhibited a concentration-dependent bell-shaped pattern of induced migration, peaking at 100 nM, and was less efficacious than NAGly (Figure 6A). CBD and AM251 both antagonized (100 nM) NAGly-induced cell migration with IC_{50} values of 28 nM and 112 nM respectively (Figure 6B). With regard to Δ^9-THC-induced migration, the IC_{50} values for CBD and AM251 were 18 nM and 79 nM respectively. Collectively, these values and the difference in starting efficacy reflect the greater potency of NAGly over Δ^9-THC as a GPR18 agonist, and CBD over AM251 as a GPR18 antagonist.

Discussion

In the current study we present evidence that the endocannabinoid system plays a role in the regulation of human endometrial cell migration and that the effect of endogenous and phytocannabinoids suggests a signalling mechanism mediated through CB_2 receptors and to a greater extent, GPR18. The most effective activator of endometrial cell migration was the AEA metabolite, NAGly, which was also a potent ligand at GPR18. We further characterized GPR18 pharmacology via p44/42 MAPK activation, demonstrating agonist profile that did not include the majority of the known CB_1 and CB_2 receptor agonists. However, our results did reveal a surprising agonist activity for Δ^9-THC at GPR18, suggesting that this orphan receptor represents an additional route for phytocannabinoid pharmacology.

Cannabinoids and endometrial migration

Recent work by Gentilini *et al*. (2010) reported that primary human endometrial stromal cells migrated towards R1-methAEA (10 μM) and that this was blocked by AM251 (10 μM), suggesting a CB_1 receptor-mediated signalling mechanism. This is in contrast to our findings with HEC-1B endometrial epithelial cells, where the data point towards migration occurring through CB_2 and GPR18 receptors, and independently of CB_1 receptors. Our HEK293-GPR18 MAPK studies show that while AM251 was a mixed CB_1/GPR18 antagonist, R1-methAEA remained a selective agonist for CB_1 receptors, supporting the conclusions of Gentilini *et al*. (2010). Stromal cells are part of the support structure of the endometrium, forming thick connective tissue, as distinct from endometrial epithelium, which is parenchymal. Therefore, differences in phenotype are likely to underlie this apparent discrepancy in regulation of migration by the endocannabinoid system. Like the endometrial epithelium, stroma also undergoes many changes to mediate the dynamic proliferation, secretion and regression events associated with the various phases of the menstrual cycle (Chard and Grudzinskas, 1994). However, Taylor *et al*. (2010) have observed notable dissimilarities in both CB_1 and CB_2 receptor immunoreactivity between stroma and epithelium in human endometrial biopsies. Maccarrone *et al*. (2000) found FAAH localized in endometrial epithelium and this is compatible with our HPLC/MS/MS data, which indicated the functional presence of a potential FAAH-dependent 'AEA-to-NAGly' conversion in HEC-1B endometrial epithelial cells.

Differences in the activity curves of AEA and NAGly-induced HEC-1B migration suggest that the increased potency of AEA is due in part to AEA potentially activating CB_2 receptors (as demonstrated by the attenuated response with pre-incubation of SR144528 and no effect of SR141716A) as well as GPR18 through the conversion of AEA to NAGly. In addition, AEA and NAGly each demonstrate the same bell-shape response with a maximization or 'ceiling effect' of migration, which does not appear to be additive as neither compound caused migration levels above ~275% of the maximum effect of oestradiol at amounts above 1 μM. Therefore, additional activation by NAGly (probably acting on GPR18) in the presence of AEA (acting on CB_2 receptors) does not increase this ceiling effect. Taken together, these results demonstrate a sophisticated role for CB_1, CB_2 receptors and GPR18 in endometrial signalling.

Novel cannabinoid pharmacology

The most current understanding of the endocannabinoid system holds that the pharmacology of endogenous and

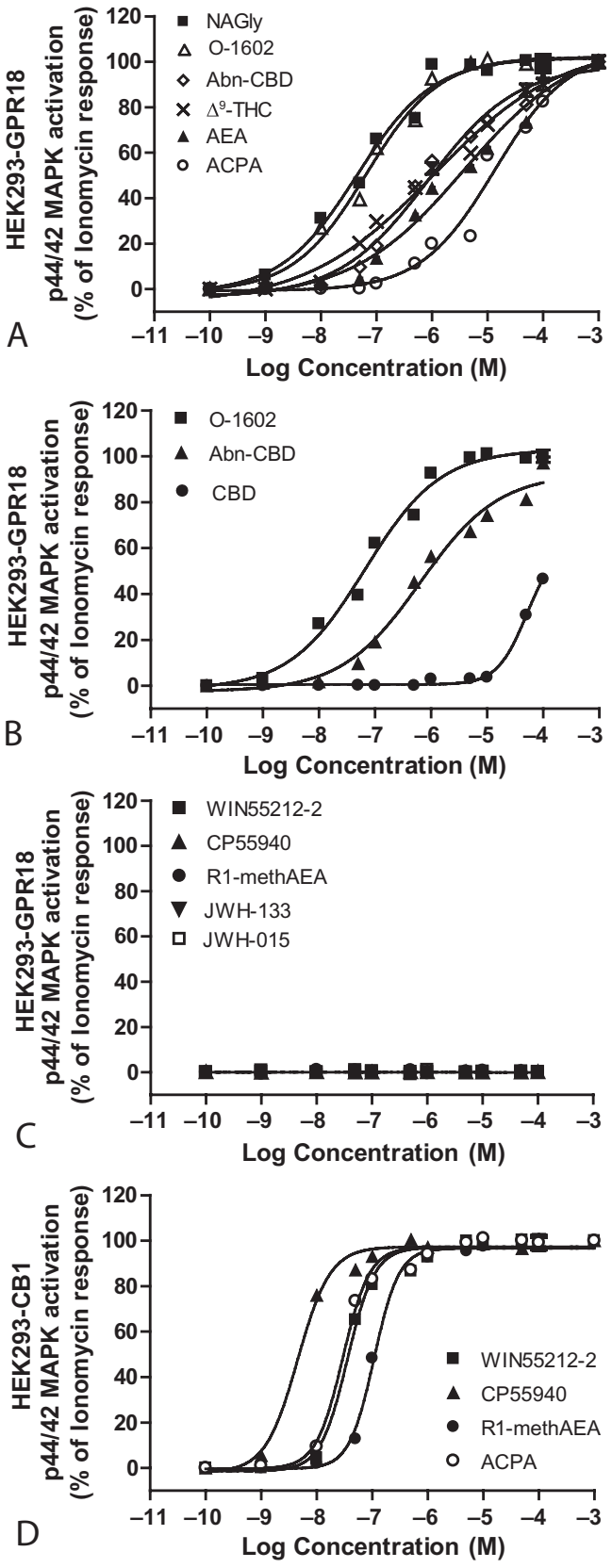

Figure 4

Concentration–response curves indicating activation of p44/42 MAPK in HEK293-GPR18 and HEK293-CB_1 cells. (A) p44/42 MAPK activation in HEK293-GPR18 cells in response to 0.1 nM–100 μM concentrations of NAGly, O-1602, Abn-CBD, Δ^9-THC, AEA and ACPA; n = 3. (B) p44/42 MAPK activation in HEK293-GPR18 cells in response to 0.1 nM–100 μM concentrations of O-1602, Abn-CBD and CBD; n = 3. (C) p44/42 MAPK activation in HEK293-GPR18 cells in response to 0.1 nM–100 μM concentrations of WIN55212-2, CP55940, R1-methAEA, JWH-133 and JWH-015; n = 3. (D) p44/42 MAPK activation in HEK293-CB_1 cells in response to 0.1 nM–100 μM concentrations of WIN55212-2, CP55940, R1-methAEA and ACPA; n = 3.

phytocannabinoids is complex. For several years, well-documented evidence has supported the existence of additional cannabinoid receptors, other than CB_1 and CB_2 receptors, contributing to the system (Begg *et al.*, 2005; Mackie and Stella, 2006; Brown, 2007; McHugh *et al.*, 2008). Our recent publication was the first to demonstrate that the $G_{i/o}$-coupled GPCR, GPR18, is one of these unknown receptors in that AEA and its metabolite NAGly exert potent control of CNS microglia (McHugh *et al.*, 2010). Moreover, in that same publication we proposed the working hypothesis that GPR18 is the molecular identity of the Abn-CBD receptor, the most prominent of the non-CB_1, non-CB_2 receptors. A portion of the data reported showed that NAGly drove MAPK (p44/42; ERK1/2) activation in GPR18-transfected HEK293 cells. Using this same expression system we screened the specificity of cannabinoid ligands including traditional CB_1 and CB_2 receptor agonists and antagonists at GPR18. In order of potency, NAGly, O-1602, Abn-CBD, Δ^9-THC, AEA and ACPA are full agonists at GPR18; CBD was a weak GPR18 partial agonist. WIN55212-2, CP55940, R1-methAEA, JWH-133 and JWH-015 had no effect. The ACPA data in Figure 4A suggested that there may be a two-site curve in the GPR18 cells, possibly reflecting two populations of GPR18 receptors (coupled and non-coupled) that have different affinity for the agonist. In order to test this, using GraphPad Prism, the fit of the ACPA data was compared between one-site curve versus a two-site curve. The *F*-test resulted in a *P*-value of <0.05, indicating that the one-site model is preferred.

It is becomingly increasingly clear that a proper understanding of GPR18 pharmacology and its physiological role is essential firstly, for an adequate understanding of the complexity of the endocannabinoid system. Secondly, to avoid misinterpretation of effects observed with ligands previously regarded as CB_1 or CB_2 receptor selective, which are also pharmacologically active at GPR18. For instance, R1-methAEA is the most potent agonist in the methanandamide series. It is approximately fourfold more potent at CB_1 receptors and more resistant to hydrolytic inactivation by FAAH, than AEA (Abadji *et al.*, 1994). These characteristics have made this ligand a convenient substitute for AEA in various tissues. However, now on the basis of our results, caution should be exercised when interpreting the outcome. Our data indicate activity for AEA but not R1-methAEA at GPR18 and that FAAH-dependent hydrolysis of AEA is likely to be an integral biosynthetic step towards the production of NAGly, which is a more potent agonist at GPR18. An appreciation of this will avoid misconstruing effects as solely CB_1 receptor- versus

Table 1

Activation of GPR18, CB_1 or CB_2 receptors stably transfected into HEK293 cells induced p44/42 MAPK phosphorylation by cannabinoids and related lipids

Compound	Activity at GPR18	EC_{50} values (95% confidence limits)	E_{max} values (95% confidence limits)
NAGly	Full agonist	44.5 nM (32.4–61.0)	101.6% (98.4–104.9)
O-1602	Full agonist	65.3 nM (49.3–86.5)	102.1% (98.9–105.3)
Abn-CBD	Full agonist	835.7 nM (579.6–1205)	98.6% (92.6–104.6)
Δ^9-THC	Full agonist	0.96 μM (0.43–2.12)	104.9% (88.7–121.2)
AEA	Full agonist	3.83 μM (2.11–6.90)	109.0% (97.3–120.8)
ACPA	Full agonist	13.5 μM (9.03–20.4)	105.5% (95.8–115.3)
CBD	Partial agonist/antagonist	51.1 μM (35.8–73.2)	61.9% (46.8–77.0)
AM251	Partial agonist/antagonist	96.4 μM (n/a)	50.3% (n/a)
WIN55212-2	None	–	–
CP55,940	None	–	–
R1-methAEA	None	–	–
JWH-133	None	–	–
JWH-015	None	–	–
SR141716A	None	–	–
SR144528	None	–	–
Compound	**Activity at CB_1**	**EC_{50} values (95% confidence limits)**	**E_{max} values (95% confidence limits)**
CP55,940	Full agonist	4.56 nM (3.60–5.79)	97.3% (94.8–98.5)
ACPA	Full agonist	29.5 nM (25.1–34.8)	98.2% (94.9–100.3)
WIN55212-2	Full agonist	35.9 nM (30.7–42.0)	97.1% (95.0–99.2)
R1-methAEA	Full agonist	108.1 nM (97.6–120.0)	96.7% (94.8–98.9)
Compound	**Activity at CB_2**	**EC_{50} values (95% confidence limits)**	**E_{max} values (95% confidence limits)**
JWH-133	Full agonist	95.7 nM (68.0–115.9)	98.1% (95.7–100.4)
JWH-015	Full agonist	207.5 nM (158.7–245.6)	98.9% (97.3–101.6)

EC_{50} and E_{max} values (percentage of p44/42 MAPK activation induced by 10 μM ionomycin) were calculated from sigmoidal concentration–response curves constructed in GraphPad Prism 4. The data represent the mean with 95% confidence limits, $n = 3$.
n/a, not available.

GPR18-mediated, especially given the antagonism of GPR18 by AM251 we also report here. It will also allow for a more nuanced use of R1-methAEA to selectively target CB_1 receptor signalling over that of GPR18 and CB_2 receptors. Thirdly, a more complete picture of GPR18 pharmacology will help to generate future hypotheses in cannabinoid research.

There are many reports of AEA and Abn-CBD activity associated with Abn-CBD receptors (also known as the 'endothelial anandamide receptor'), that are either insensitive to SR141617A antagonism (Mukhopadhyay *et al.*, 2002; Walter *et al.*, 2003; Milman *et al.*, 2005; O'Sullivan *et al.*, 2005; McHugh *et al.*, 2010) or require substantially greater concentrations than those required to block CB_1 receptors (White and Hiley, 1998; Járai *et al.*, 1999; Wagner *et al.*, 1999; McHugh *et al.*, 2008). Our data showed that SR141716A had no effect on migration of HEC-1B cells (Figure 1C).

The lack of consistency for SR141716A antagonism at Abn-CBD receptors may be explained as a product of its affinity for Abn-CBD receptors and the number that need to be blocked in order to observe a reduction in signalling, which will in turn vary according to the degree of receptor reserve in any given tissue. AM251 is structurally very similar to SR141716A. In light of this, we hypothesized that AM251 may be able to antagonize GPR18 receptors, where SR141716A failed to do so. SR141617A and AM251 are both biarylpyrazole antagonists. In AM251, the *p*-chloro group attached to the phenyl substituent at C-5 of the pyrazole ring of SR141716A is replaced with a *p*-iodo group – essentially a halogen substitution (Lan *et al.*, 1999). Structure–activity studies where comparable halogen substitutions were made on the vanillyl moieties of the TRPV1 agonists resiniferatoxin and nordihydrocapsaicin, have yielded potent TRPV1 antagonists (Wahl

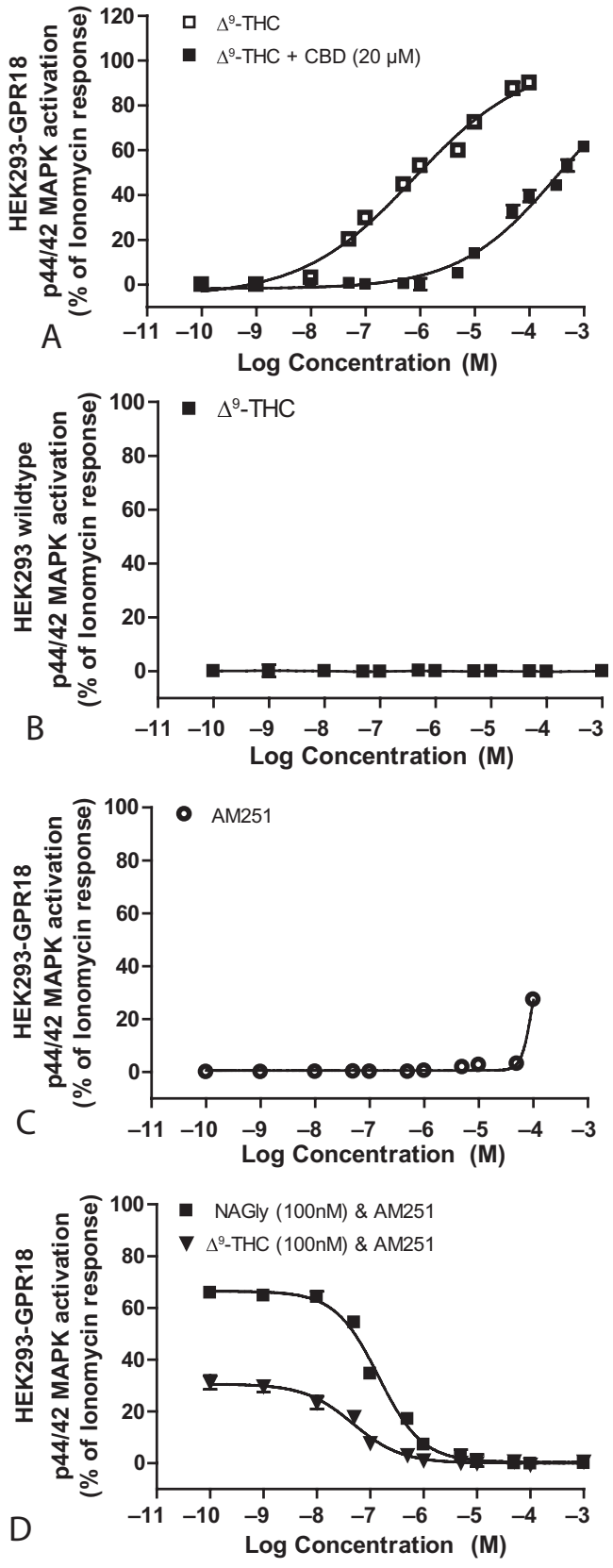

Figure 5

Concentration–response curves indicating activation of p44/42 MAPK in HEK293-GPR18 and HEK293 wildtype cells. (A) p44/42 MAPK activation in HEK293-GPR18 cells in response to 0.1 nM–100 μM concentrations of Δ^9-THC alone and 0.1 nM–1 mM Δ^9-THC + 20 μM CBD; n = 3. (B) HEK293 wildtype cell p44/42 MAPK activation in response to 0.1 nM–100 μM concentrations of Δ^9-THC; n = 3. (C) p44/42 MAPK activation in HEK293-GPR18 cells in response to 0.1 nM–100 μM concentrations of AM251; n = 3. (D) p44/42 MAPK activation in HEK293-GPR18 cells in response to 100 nM NAGly + 0.1 nM–100 μM AM251 and 100 nM Δ^9-THC + 0.1 nM–100 μM AM251; n = 3.

et al., 2001; Appendino *et al.*, 2003). In addition, Liu and Simon (1997) found that the inhibitory potency of TRPV1 antagonists correlated directly with the size of the halogen substituent (I > Br > Cl) and inversely with its electronegativity. Based on these data, and in order to further test our hypothesis that GPR18 is the molecular identity of the Abn-CBD receptor, we predicted that AM251 would be a more potent antagonist at GPR18 than SR141716A. Our results are in support of this. AM251 antagonized NAGly and Δ^9-THC activation of p44/42 MAPK in HEK293-GPR18 cells with IC_{50} values of ~144 nM and ~47 nM respectively (Figure 5D). AM251 also antagonized NAGly and Δ^9-THC-induced migration of HEC-1B cells, where SR141716A had no effect (Figures 1C and 6B,C); AM251's IC_{50} values here were ~ 112 nM and ~ 80 nM respectively. Furthermore, the IC_{50} values for AM251 antagonism of GPR18 (Abn-CBD receptors) are lower than the reported IC_{50} for SR141716A, of ~ 600 nM at Abn-CBD receptors (Jung *et al.*, 1997; Bukoski *et al.*, 2002).

In conclusion, the discovery of the endocannabinoid system began with the identification of a single GPCR, the CB_1 receptor and the first endogenous ligand, anandamide. However, a very few additional components have accrued over the last two decades to produce a small group of endocannabinoid receptors and ligands. Recent discussions have centred on what it means to be a member of the 'cannabinoid' family and whether or not the levels of inclusion and exclusion are beneficial in terms of getting to a better understanding of the science related to how the phytocannabinoids either mimic or interfere with endogenous mammalian signalling systems (see Pertwee *et al.*, 2010). Here, we provide data that the $G_{i/o}$-coupled GPCR, GPR18, was activated by Δ^9-THC and additional data showing that CBD acted as an antagonist at this same receptor. These results demonstrate that greater concentrations of Δ^9-THC are required to activate GPR18 receptors, than of CBD to produce GPR18 antagonism, a difference that is likely to affect the therapeutic outcome of existing pharmacotherapies that combine both Δ^9-THC and CBD.

We also provide evidence that an endogenous metabolite of anandamide, NAGly, mimicked the effects of Δ^9-THC in driving migration of the human endometrial cell line, HEC-1B, which was also blocked by <100 nM of CBD. These data potentially explain the 'idiosyncratic' outcomes from some previous studies in the field in which the effects of CB_1 and CB_2 receptors were unable to account for the observed phenomena.

The endocannabinoid system branch of neuroscience research is still evolving; however, it is already clear that it

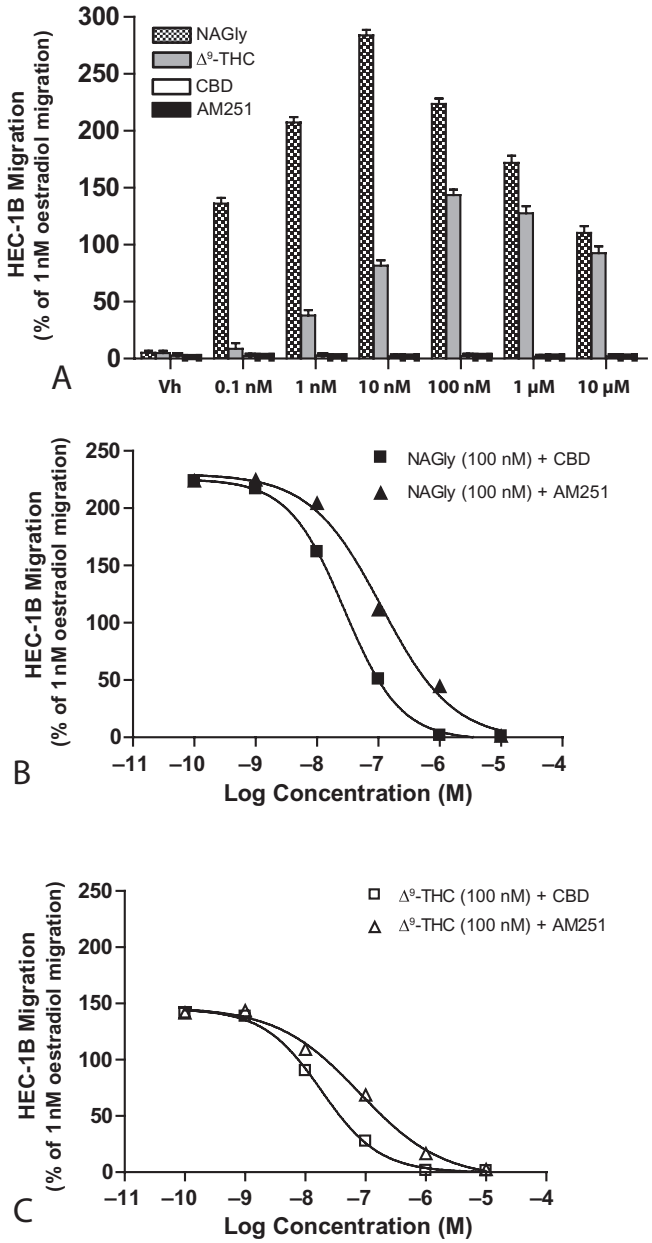

Figure 6

Δ^9-THC and NAGly-induced HEC-1B endometrial cell migration is antagonized by AM251 and CBD. (A) HEC-1B cell migration in response to basal conditions; vh (0.1% DMSO); 0.1 nM–10 μM concentrations of NAGly, Δ^9-THC, CBD and AM251; n = 3. (B) HEC-1B cell migration in response to basal conditions; 100 nM NAGly + 0.1 nM–10 μM CBD; 100 nM NAGly + 0.1 nM–10 μM AM251; n = 3. (C) HEC-1B cell migration in response to basal conditions; 100 nM Δ^9-THC + 0.1 nM–10 μM CBD; 100 nM Δ^9-THC + 0.1 nM–10 μM AM251; n = 3.

powerfully regulates neuronal, vascular, immune and reproductive functions. An understanding of the expression, function and regulation of the hitherto unidentified cannabinoid receptors such as GPR18, their molecular interactions with endogenous ligands, and how phytocannabinoids play a role with their signalling is vital if we are to comprehensively assess the function of the cannabinoid signalling system in human health and disease.

Acknowledgements

This work was supported by NIH DA018224.

Conflicts of interest

The authors have no conflicts of interests.

References

Abadji V, Lin S, Taha G, Griffin G, Stevenson LA, Pertwee RG *et al.* (1994). (R)-Methanandamide: a chiral novel anandamide possessing higher potency and metabolic stability. J Med Chem 37: 1889–1893.

Acconcia F, Barnes CJ, Kumar R (2006). Estrogen and tamoxifen induce cytoskeletal remodeling and migration in endometrial cancer cells. Endocrinology 147: 1203–1212.

Alexander SPH, Mathie A, Peters JA (2011). Guide to Receptors and Channels (GRAC), 5th Edition. Br J Pharmacol 164 (Suppl. 1): S1–S324.

Appendino G, Harrison S, De Petrocellis L, Daddario N, Bianchi F, Moriello AS *et al.* (2003). Halogenation of a capsaicin analogue leads to novel vanilloid TRPV1 receptor antagonists. Br J Pharmacol 139: 1417–1424.

Begg M, Mo F-M, Offertaler L, Batkai S, Pacher P, Razdan RK *et al.* (2003). G protein-coupled endothelial receptor for atypical cannabinoid ligands modulates a $Ca2^+$-dependent K^+ current. J Biol Chem 278: 46188–46194.

Begg M, Pacher P, Batkai S, Osei-Hyiaman D, Offertaler L, Fong MM *et al.* (2005). Evidence for novel cannabinoid receptors. Pharmacol Ther 106: 133–145.

Bradshaw HB, Rimmerman N, Hu SS, Benton VM, Stuart JM, Masuda K *et al.* (2009). The endocannabinoid anandamide is a precursor for the signaling lipid N-arachidonoyl glycine by two distinct pathways. BMC Biochem 10: 14.

Brown AJ (2007). Novel cannabinoid receptors. Br J Pharmacol 152: 567–575.

Bukoski RD, Batkai S, Járai Z, Wang Y, Offertaler L, Jackson WF *et al.* (2002). CB1 receptor antagonist SR141716A inhibits CA^{2+}-induced relaxation in CB1 receptor-deficient mice. Hypertension 39: 251–257.

Bulletti C, Coccia ME, Battistoni S, Borini A (2010). Endometriosis and infertility. J Assist Reprod Genet 27: 441–447.

Burstein SH, Rossetti RG, Yagen B, Zurier RB (2000). Oxidative metabolism of anandamide: eScholarship@UMMS. Prostaglandins Other Lipid Mediat 61: 29–41.

Chard T, Grudzinskas JG (1994). The Uterus. Cambridge University Press: New York. ISBN: 9780521424530.

Derocq JM, Jbilo O, Bouaboula M, Segui M, Clere C, Casellas P (2000). Genomic and functional changes induced by the activation of the peripheral cannabinoid receptor CB2 in the promyelocytic cells HL-60. Possible involvement of the CB2 receptor in cell differentiation. J Biol Chem 275: 15621–15628.

Devane WA, Hanus L, Breuer A, Pertwee RG, Stevenson LA, Griffin G *et al.* (1992). Isolation and structure of a brain constituent that binds to the cannabinoid receptor. Science 258: 1946–1949.

Fujimoto J, Hori M, Ichigo S, Morishita S, Tamaya T (1996). Estrogen activates migration potential of endometrial cancer cells through basement membrane. Tumour Biol 17: 48–57.

Gentilini D, Besana A, Vigano P, Dalino P, Vignali M, Melandri M *et al.* (2010). Endocannabinoid system regulates migration of endometrial stromal cells via cannabinoid receptor 1 through the activation of P13K and ERK1/2 pathways. Fertil Steril 93: 2588–2593.

Huang SM, Bisogno T, Petros TJ, Chang SY, Zavitsanos PA, Zipkin RE *et al.* (2001). Identification of a new class of molecules, the arachidonyl amino acids, and characterization of one member that inhibits pain. J Biol Chem 276: 42639–42644.

Járai Z, Wagner JA, Varga K, Lake KD, Compton DR, Martin BR *et al.* (1999). Cannabinoid-induced mesenteric vasodilation through an endothelial site distinct from CB1 or CB2 receptors. Proc Natl Acad Sci U S A 96: 14136–14141.

Jung M, Cassi R, Rinaldi-Carmona M, Chardenot P, Le Fur G, Soubre P *et al.* (1997). Characterization of CB1 receptors on rat neuronal cell cultures: binding and functional studies using the selective receptor antagonist SR141716A. J Neurochem 68: 402–409.

Kitawaki J, Kado N, Ishihara H, Koshiba H, Kitaoka Y, Honjo H (2002). Endometriosis: the pathophysiology as an estrogen-dependent disease. J Steroid Biochem Mol Biol 83: 149–155.

Klinger FG, Battista N, De Felici M, Maccarrone M (2006). Stage-variations of anandamide hydrolase activity in the mouse uterus during the natural oestrus cycle. J Exp Clin Assist Reprod 3: 3.

Kohno M, Hasegawa H, Inoue A, Muraoka M, Miyazaki T, Oka K *et al.* (2006). Identification of N-arachidonylglycine as the endogenous ligand for orphan G-protein-coupled receptor GPR18. Biochem Biophys Res Commun 347: 827–832.

Lan R, Liu Q, Fan P, Lin S, Fernando SR, McCallion D *et al.* (1999). Structure-activity relationships of pyrazole derivatives as cannabinoid receptor antagonists. J Med Chem 42: 769–776.

Liu L, Simon SA (1997). Capsazepine, a vanilloid receptor antagonist, inhibits nicotinic acetylcholine receptors in rat trigeminal ganglia. Neurosci Lett 228: 29–32.

Maccarrone M, De Felici M, Bari M, Klinger F, Siracusa G, Finazzi-Agro A (2000). Down-regulation of anandamide hydrolase in mouse uterus by sex hormones. Eur J Biochem 267: 2991–2997.

Maccarrone M, Bisogno T, Valensise H, Lazzarin N, Fezza F, Manna C *et al.* (2002). Low fatty acid amide hydrolase and high anandamide levels are associated with failure to achieve an ongoing pregnancy after IVF and embryo transfer. Mol Hum Reprod 8: 188–195.

Mackie K, Stella N (2006). Cannabinoid receptors and endocannabinoids: evidence for new players. AAPS J 8: E298–E306.

McHugh D, Hu SS, Rimmerman N, Juknat A, Vogel Z, Walker JM *et al.* (2010). N-arachidonoyl glycine, an abundant endogenous lipid, potently drives directed cellular migration through GPR18, the putative abnormal cannabidiol receptor. BMC Neurosci 11: 44.

Pertwee RG, Howlett AC, Abood ME, Alexander SPH, Di Marzo V, Elphick MR *et al.* (2010). International Union of Basic and Clinical Pharmacology. LXXIX. Cannabinoid receptors and their ligands: beyond CB_1 and CB_2. Pharmacol Rev 62: 588–631.

Schmid PC, Paria BC, Krebsbach RJ, Schmid HH, Dey SK (1997). Changes in anandamide levels in mouse uterus are associated with uterine receptivity for embryo implantation. Proc Natl Acad Sci U S A 94: 4188–4192.

Sheskin T, Hanus L, Slager J, Vogel Z, Mechoulam R (1997). Structural Requirements for Binding of Anandamide-Type Compounds to the Brain Cannabinoid Receptor. J Med Chem 40: 659–667.

Song ZH, Zhong M (2000). CB1 cannabinoid receptor-mediated cell migration. J Pharmacol Exp Ther 294: 204–209.

Sun X, Dey SK (2008). Aspects of endocannabinoid signaling in periimplantation biology. Mol Cell Endocrinol 286 (Suppl. 1): S3–S11.

Talbi S, Hamilton AE, Vo KC, Tulac S, Overgaard MT, Dosiou C *et al.* (2006). Molecular phenotyping of human endometrium distinguishes menstrual cycle phases and underlying biological processes in normo-ovulatory women. Endocrinology 147: 1097–1121.

Tallarida RJ, Jacob LS (1979). The dose-response relation in pharmacology, Springer-Verlag: New York. ISBN 0387904158.

Taylor AH, Abbas MS, Habiba MA, Konje JC (2010). Histomorphometric evaluation of cannabinoid receptor and anandamide modulating enzyme expression in the human endometrium through the menstrual cycle. Histochem Cell Biol 133: 557–565.

Wagner JA, Varga K, Jarai Z, Kunos G (1999). Mesenteric vasodilation mediated by endothelial anandamide receptors. Hypertension 33: 429–434.

Wahl P, Foged C, Tullin S, Thomsen C (2001). Iodo-resiniferatoxin, a new potent vanilloid receptor anatagonist. Mol Pharmacol 59: 9–15.

Walter L, Franklin A, Witting A, Wade C, Xie Y, Kunos G *et al.* (2003). Nonpsychotropic cannabinoid receptors regulate microglial cell migration. J Neurosci 23: 1398–1405.

Xiao AZ, Zhao YG, Duan EK (2002). Expression and regulation of the fatty acid amide hydrolase gene in the rat uterus during the estrous cycle and peri-implantation period. Mol Hum Reprod 8: 651–658.

Supporting information

Additional Supporting Information may be found in the online version of this article:

Table S1 Activation of HEK293 wildtype cell induced p44/42 MAPK phosphorylation by cannabinoids and related lipids. 'None' means that there was no significant difference in response to that of vehicle (Vh; 0.1% DMSO) alone. $n = 3$

Please note: Wiley-Blackwell are not responsible for the content or functionality of any supporting materials supplied by the authors. Any queries (other than missing material) should be directed to the corresponding author for the article.